J. Eng. Technol. Sci., Vol. 54, No. 4, 2022, 220407

Microwave-assisted Synthesis of Functionalized Multiwalled Carbon Nanotube–Titanium Dioxide Hybrid Structure and Photodegradation

Yuyun Irmawati[1,*], Shofia Manzalini[2], Bambang Sugeng[1], Sudirman[1], Harayasu Asahara[3] & Rike Yudianti[1]

[1]Research Center for Advanced Materials, National Research and Innovation Agency (BRIN), Kawasan Puspiptek, Gd. 440-441, Serpong, Tangerang Selatan 15314, Indonesia
[2]Physics Department, UIN Sunan Gunung Djati, Jalan A.H. Nasution Rd., Cibiru-Bandung 40614, Indonesia
[3]Department of Applied Chemistry, Graduate School of Engineering, Osaka University, Suita, Osaka, Japan
*E-mail: yuyun.irmawati@brin.go.id

Highlights:

- Microwave-heating provides a fast, cost-effective and clean approach to synthesis of hybrid TiO_2/functionalized MWCNT.
- The mass ratio of f-MWCNT to TiO_2 precursor influences the phase transformation and crystallite size of TiO_2.
- The crystalline phase of TiO_2 is closely related to its photocatalytic activity

Abstract. Decoration of a functionalized multiwalled carbon nanotube (f-MWCNT) surface with titanium dioxide (TiO_2) was designed to improve its photocatalytic degradation performance. Structural decoration was achieved by microwave heating at various mass ratios (1:2; 1:4; 1:8; 1:16 wt.%) of titanium (IV) isopropoxide as precursor. The hybrid structure of TiO_2/f-MWCNT was characterized by scanning electron microscope and transmission electron microscope (TEM). The crystallite form of the TiO_2 nanoparticles was further studied by X-ray diffraction (XRD) and HR–TEM. We report the conformation of high-density TiO_2 coated on an f-MWCNT surface at a mass ratio of 1:16 wt.%. XRD analysis revealed a structural transformation from mixture phase (anatase–brookite) at mass ratios of 1:2 and 1:4 wt.% to fully anatase phase for mass ratios of 1:8 and 1:16 wt.%. The transformation was also confirmed by selected area electron diffraction (SAED) and HR–TEM analysis. Our results showed that anatase phase plays a significant role in photodegradation activity.

Keywords: *anatase; brookite; f-MWCNT; microwave heating technique; photocatalytic.*

1 Introduction

Carbon nanotubes (CNT) possess extraordinary mechanical, electronic, optical and thermal properties [1] due to their structure. These properties allow CNT to

Received May 23rd, 2021, Revised August 8th, 2021, Accepted for publication March 25th, 2022.
 ISSN: 2337-5779,
DOI: 10.5614/j.eng.technol.sci.2022.54.4.7

be a functional material in various applications of nanocomposites, such as super capacitors, biosensors, tissue engineering and renewable energy, including solar cells and fuel cells [1-4].

Titanium oxide (TiO_2) is one of many light-metal oxides that are active when used for solar energy conversion. This material is nontoxic, low-cost, thermally stable and possesses unique electronic and optical properties [5,6]. The phase composition of TiO_2 nanomaterials is one of the factors that strongly influence their photocatalytic activity. Anatase of TiO_2 has been largely used as active material for photocatalysis. It has a wide bandgap (3.2 eV) and more free electrons than rutile crystals [7]. Its quantum efficiency in photocatalytic reactions, however, is limited due to its large band gap and high rate of electron-hole recombination. Therefore, it is necessary to expand the spectral absorption band of TiO_2, to increase its photocatalytic efficiency.

Currently deposition of metal or metal oxide onto CNT is a popular but challenging research area for various applications. Utilization of hybrid nanocomposites based on CNT [8-10] has been considered as a method to enlarge the absorption region of light harvesting materials for improving the overall efficiency of the photocatalytic process [11]. Multiwalled carbon nanotubes (MWCNT) with a large surface area are particularly suited for accepting electrons from TiO_2, reducing the accumulation of electrons in the TiO_2 nanoparticles [12,13], increasing electron transfer, and decreasing charge recombination [14].

Procedures for synthesis of CNT/TiO_2 have been commonly reported, including those using the sol-gel method [15,16], mechanical techniques [15,17], and hydrothermal techniques [18,19]. However, these methods are known to be time consuming, requiring multiple steps, to be costly due to high-temperature treatment, and to induce structural damages to the nanotubes. In this study, we present a fast, cost-effective and clean approach to the synthesis of TiO_2/functionalized MWCNT (f-MWCNT) nanocomposites by microwave irradiation, which is regarded as a safe 'green chemistry' technique. Microwave irradiation allows rapid synthesis by effectively introducing energy to the system.

2 Experimental Method

2.1 Materials

MWCNT was purchased from Chengdu Alpha Nano Tech Co. Ltd., with a purity of 95%, an outer diameter of 20 to 50 nm, and a length of about 5 μm. Titanium tetra-isopropoxide/TTIP (0.96 g/mL) as titanium precursor and methylene blue (MB) were purchased from Sigma Aldrich. Sodium dodecyl sulphate (SDS; 99%)

and ethanol were purchased from Merck as dispersant and reducing agent, respectively.

2.2 Microwave Synthesis of f-MWCNT/TiO_2 Hybrids

f-MWCNT was synthesized using a polyol procedure as reported by Yudianti, *et al.* [20,21]. TTIP ($Ti[OCH(CH_3)_2]_4$) was dissolved in ethanol (50 mL) and then dispersed through ultrasonication for 3 h at room temperature [20]. The f-MWCNT (10 mg) was dispersed in 50-mL ethanol containing SDS (5 mg) for 3 h at room temperature. The f-MWCNT solution was added drop-wise to the TTIP solution with stirring for 2 h. The mass ratios of the f-MWCNT/TTIP components are reported in Table 1. A hybridization reaction occurred under microwave heating, with energy introduced for 6 min, after which the suspended solution showed a color change from black and white to dark grey. After microwave heating, the f-MWCNT/TiO_2 nanocomposite was annealed stepwise at 100 °C (24 h) and subsequently calcinated at 500 °C (1h).

Table 1 Composition of the f-MWCNT/TiO_2 nanocomposites.

Sample	Materials hybrids	Ratio (wt.%)
A	f-MWCNT:TTIP	1:2
B	f-MWCNT:TTIP	1:4
C	f-MWCNT:TTIP	1:8
D	f-MWCNT:TTIP	1:16

2.3 Structure and Morphological Surface Analysis

The morphological surface and distribution of TiO_2 on the *f*-MWCNT surface were observed by SEM (JEOL JSM-IT300) at 15 kV and TEM (FEI Tecnai G2 20 S-Twin) at 200 kV, respectively. The TEM samples were dispersed in ethanol, then dropped onto Cu-grid carbon before drying at room temperature. Chemical composition analysis was performed using XPS (JEOL JPS-9010) with an Mg Kα 1243.6-eV radiation source. We used sample D as representative of the nanocomposite materials for XPS measurement. Powder sample D was stuck on indium paste prior to performing the measurement.

The nanocomposite structures with various mass ratios were characterized by XRD (PANalytical Empyrean Philips) using Cu-Kα with a wavelength (λ) of 1.54 Å at 30 mA and 40 kV. The phase composition of TiO_2 crystallite was characterized by XRD–Rietveld refinement and selected-area electron diffraction (SAED) analysis. The mean crystallite size was calculated with the highest peak using Scherrer's equation for a given phase (q) and full width at half maximum (FWHM; β) after correcting the instrumental broadening with the following Eq. (1):

$$D = 0.89\,\lambda / (\beta \cos(q)) \quad (1)$$

2.4 Photocatalytic Activity Test

Photocatalytic activity was evaluated by measuring the decomposition of MB (10 μM) under UV irradiation. Commercially available UV light (15W, λ = 365 nm) was used in the experiment. A suspension was prepared by mixing 1.2 mg of photocatalyst with 50 mL of MB solution. Before measurement, the suspension was magnetically stirred in a dark chamber until its absorbance became constant to ensure that physical adsorption would not play any role in reducing the concentration of MB. Changes of the concentration of MB were observed based on its characteristic absorption (A_t) at 658 nm using a UV-vis spectrometer. Thus, the photo-degradation efficiency was obtained with the following Eq. (2):

$$R = (Ao - At) / Ao \times 100\% \quad (2)$$

3 Results and Discussion

3.1 Morphological and Structural Analysis

In general, the crystallographic structure of an inorganic constituent is analyzed by XRD. The diffraction patterns of the f-MWCNT (Figure 1) show two main peaks, which are the highest peaks as a carbon diffraction plane from (002) (2θ = 26.1°) and a carbon diffraction plane from (100) (2θ = 44.3°) of the hexagonal structure (ICDD No. 00-075-1621). The diffraction patterns of the hybrid nanocomposites were observed from samples A-D when TiO_2 coated the f-MWCNT surface. Some of the diffraction peaks corresponding to the crystalline phases of TiO_2 were comparable to those recorded for the standard crystals of anatase (ICDD No. 00-021-1272), rutile (ICDD 00-021-1276), and brookite (ICDD No. 00-029-1360). For samples A-D, the carbon diffraction of the f-MWCNT peak at approximately $2\theta = 26.1°$ could not be clearly detected due to the possibility of overlapping with the high intensity of the TiO_2 peak [22].

According to our XRD–Rietveld refinement, samples A-B contained mixed phases of anatase and brookite, represented by the highest diffraction plane (101) of anatase (at 2θ = 25.48°) and (111) brookite, respectively. This may coincidentally overlap with the lattice diffraction of the (002) hexagonal carbon. The two known titania phases, anatase (tetragonal) and brookite (orthorhombic), were obtained via XRD and Rietveld refinement. The shoulder peak of samples A-B disappeared when the TTIP concentration increased, and a gradual transformation to complete anatase could be observed with respect to diffraction planes of (101), (004), (200), (105), (211) and (204), which is in good agreement with the anatase standard ICDD 00-021-1272 [23].

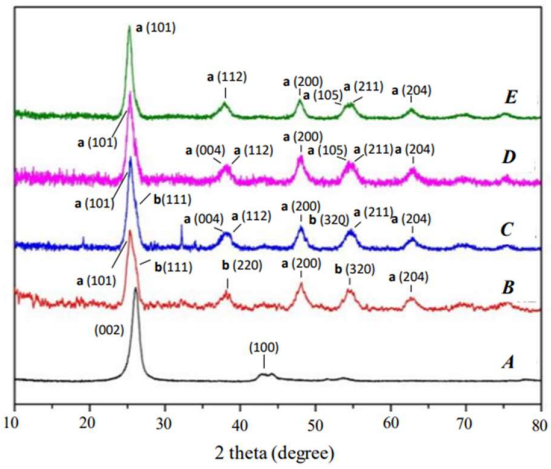

Figure 1 X-ray diffraction patterns of the MWCNT-TTIP nanocomposites at different ratios: (A) f-MWCNT, (B) sample A, (C) sample B, (D) sample C, (E) sample D.

For low mass ratio nanocomposites (samples A and B), anatase is the main contributor with approximately 71 and 89 wt.%, while brookite presents a small contribution of approximately 29 and 11 wt.%, respectively. The crystallite size was calculated using the Sherrer equation; the highest intensity was used for measuring the FWHM of the main peak. Gradual increase of the anatase-crystallite size resulted in sizes of approximately 7.0, 7.5, 7.9 and 10.2 nm for samples A, B, C, and D, respectively. The brookite-crystallite size is also indicated for sizes of 6.25 and 10.5 nm, respectively, for samples A and B. X-ray analysis revealed that the structural transformation from mixed phase (samples A-B) to fully anatase phase (samples C-D) was influenced by the precursor concentration when all the samples were heated to 500 °C. Previous studies also demonstrated crystal transformation could be achieved via heating treatment [19,24] and acid-assisted hydrothermal treatment [25].

From the SEM images (Figure 2), the morphology of the hybrid f-MWCNT/TiO_2 showed different distribution levels of TiO_2 nanoparticles on the f-MWCNT sidewall at different mass ratios of TTIP precursor. Sample A showed a continuous polymer matrix covering the nanotube network. Some agglomerated TiO_2 particles can clearly be seen at a few different locations in the image. When the TTIP concentration increased, an aggregate of white TiO_2 particles tended to grow randomly on the carbon fiber network and the continuous matrix disappeared (sample B). Nanoparticles growing on the surface of nanotubes thickens the nanotubes, which can also clearly be seen in the SEM image.

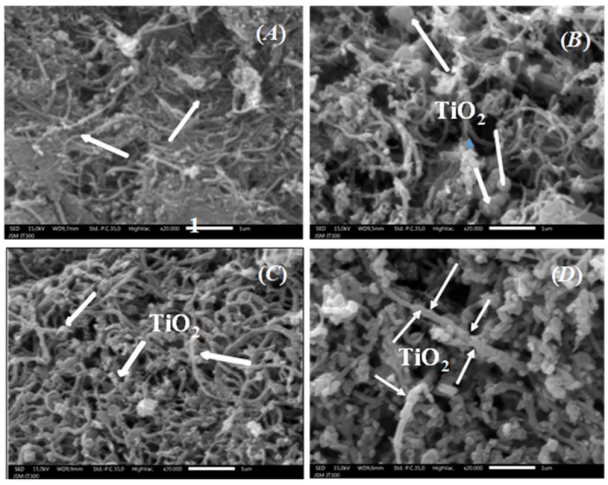

Figure 2 SEM images of TiO_2 on the CNT sidewall with different mass ratios: (A) sample A, (B) sample B, (C) sample C, and (D) sample D.

Moreover, TiO_2-nanoparticles growing on the sidewall were observed in the TEM images (Figure 3). Deposition of TiO_2 on the carbon support indicates a successfully formed hybrid structure. Samples B, C and D were selected as representative microscopic nanocomposites and compared with the f-MWCNT with a diameter of 32.0 nm.

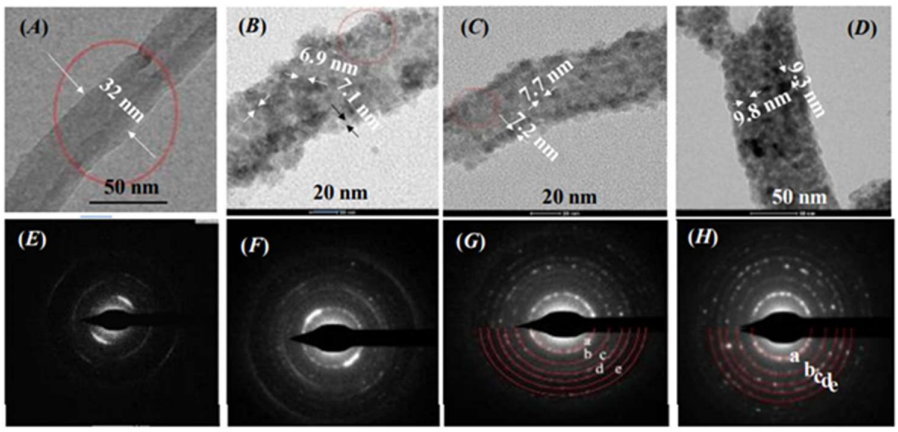

Figure 3 TEM images: (A) f-MWCNT, (B) sample B, (C) sample C, (D) sample D; SAED patterns of the MWCNT-TiO_2 nanocomposites: (E) f-MWCNT, (F) sample B, (G) sample C, (H) sample D.

The TiO_2 nanoparticles of sample B comprised a considerable number of heterogeneous structures with sizes of approximately 7.2 nm on average, which was less than those of other samples. An increase in the mass ratio of TTIP allows the nanoparticles to grow uniformly to an average size of 7.8 nm on the sidewall of the nanotube, as shown by sample C. Highly dense and large-sized spherical TiO_2 nano-particles with a size of approximately 9.4 nm were observed in sample D.

SAED patterns corresponding to the crystallographic structure of the hybrid nanocomposite are shown in Figures 3 (E, F, G and H). Spot-diffraction patterns of individual f-MWCNT can be observed in Figure 3E. Spot-diffraction patterns related to the multi-wall structure, which is perpendicular to the nanotube axis, were identified. The spot distribution provides information about the inter-layer distances between the f-MWCNT walls. The ring spot diffraction patterns from samples B, C, and D reveal crystal transformation from mixed to fully anatase phase. A polycrystalline structure is indicated by diffused spotting at low concentrations, which gradually transforms to a state of high crystallinity with high brightness of the spot pattern (sample D). This trend suggests that the mass ratio between f-MWCNT and the precursor affects the crystallite size and phase of TiO_2. Similarly, phase transformation can be observed with respect to the mass ratio of TiO_2 and benzoic acid [26]. Another discussion is related to the effect of molar ratio on the photocatalytic activity of TiO_2 thin film [27,28].

From HR-TEM image (Figure 4), the inter-planar spacings of sample B were 3.541 and 3.568 Å, which corresponds to the d_{101} of tetragonal TiO_2 (anatase). Inter-planar spacings of 3.480 and 3.512 Å were identified from sample B, which correspond to the d_{111} and d_{120} of orthorhombic TiO_2 (brookite).

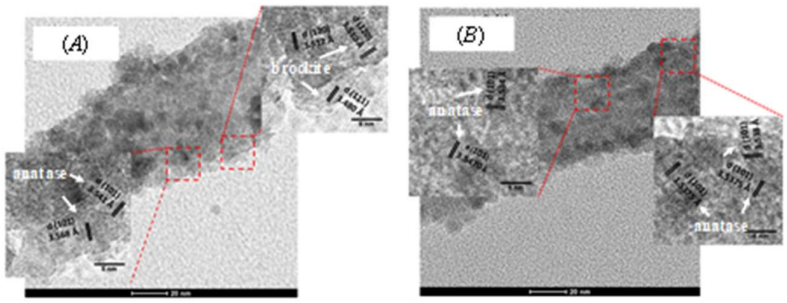

Figure 4 HR–TEM images of the TiO_2/f-MWCNT nanocomposite: (A) sample B; (B) sample C.

This is in accordance with the XRD profile of sample B, in which mixed phases were observed. Furthermore, the particle sizes and their distribution were

statistically measured using the Image-J software. We obtained average particle sizes of 7.17 ± 2.01, 7.88 ± 1.99 and 9.38 ± 1.77 nm for samples B, C and D, respectively. These particle sizes are also in agreement with the XRD–Rietveld refinement of TiO_2 anatase.

3.2 UV-vis Spectroscopy Analysis

Photocatalytic activities of the TiO_2/MWCNT nanocomposite were studied using UV absorption, photodegradation efficiency, and kinetic rate constant (Figure 5). As control, MB degradation was also included, representing the absorption spectra of dyes under UV light irradiation without photocatalytic material (Figure 5(a)). Changes in absorbance at 658 nm as the wavelength of MB characteristic peaks were used to observe progressive dye decomposition by increasing the exposure time up to 120 min. Prior to photodegradation measurement, changes in the spectra due to physical adsorption were also investigated. As illustrated in Figure 5(d), after dark conditioning, there was a decrease in the A_t/A_0 ratio for samples A, B, C by about 15, 5, and 33%, respectively. This indicates a strong influence of f-MWCNT's ability to adsorb MB molecules. MB molecules can be adsorbed through π-π stacking interactions of the aromatic groups. Meanwhile, from Figure 5(d), sample D did not show dye absorption after dark conditioning. The constant A_t/A_0 for sample D is attributed to dense growth of TiO_2 on the f-MWCNT's surface, reducing the accessibility of dye molecules to be adsorbed by the f-MWCNT.

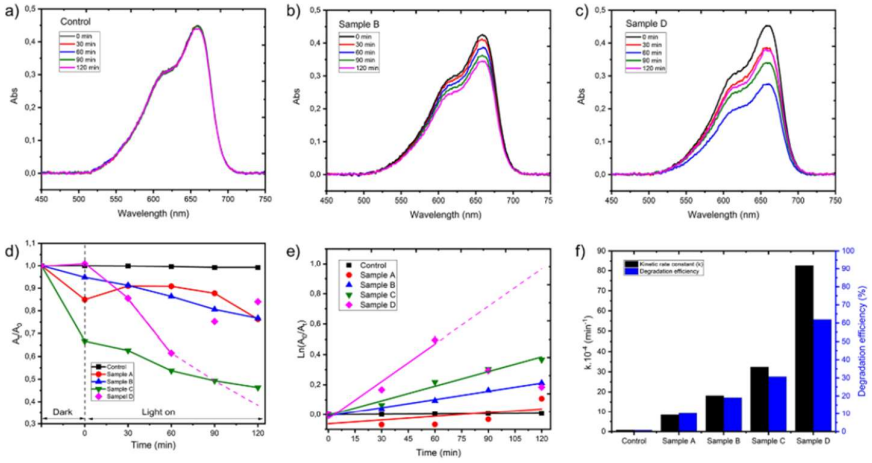

Figure 5 UV-vis absorption spectra for sample without photocatalyst (a), sample B (b), and sample D (c). Adsorption and photodegradation of MB (d) and kinetic rate constant and degradation efficiency (e and f) of the photocatalyst samples.

In Figure 5(e), the kinetic plots of ln (A_0/A_t) against time of irradiation (t) of all samples show a gradual increase in rate constant from 8 to 32 x10^{-4} min^{-1} for samples A-C. The value spiked to the highest rate constant (83 x10^{-4} min^{-1}) in sample D. This trend could be related to the predominant existence of pure anatase phase and massive growth of TiO_2 particles on the f-MWCNT surface for sample D. Since the rate of MB degradation via heterogeneous photocatalytic degradation is determined by the fraction of the catalyst surface covered by synthetic dye [29], a high kinetic rate constant would also result in an increase in photodegradation efficiency. Form Figure 5(f), sample D showed adequate photodegradation efficiency at about 61 %, compared to only 15% for sample A. The dominance of anatase phase in the photoactivity is similar to a previous study, which found that anatase exhibited two times higher catalytic activity compared to rutile phase [30]. In addition, according to Carrera, *et al.* [31], anatase is thermodynamically stable at sizes of less than 11 nm. Regarding this, sample D had a particle size of 9.38 nm.

3.2.1 X-Ray Photoelectron Spectroscopy Analysis

In addition, the TiO_2/f-MWCNT surface was observed by TEM, and the binding energies of the nanocomposite elements were verified by other techniques. XPS measurement analysis is a technique to identify the binding energy of elements that exist within the nanocomposite (Figure 6). We used sample D as representative for the nanocomposite materials. Based on the spectrum scan, the nanocomposites contained C, O and Ti elements consisting of C 1s, O 1s and Ti 2p regions. The C 1s spectrum was deconvoluted into complex peaks at 284.5, 285.9, 286.3 and 289.1 eV, which were assigned to (C–C), (C–O), (C=O) and (–COOH) groups, respectively. Oxidation of MWCNT resulted in reactive groups, i.e., (C–C), (C–O), (C=O) and (–COOH) on polar surfaces, which are ideal for adsorbing TiO_2 nanoparticles. The ethanol used during the synthesis facilitates the adsorption of precursor on the f-MWCNT, where nucleation and crystallization of TiO_2 nanoparticles occurs on the f-MWCNT's surface.

The existence of reactive groups on the f-MWCNT's surface causes TiO_2 binding, such as a thin layer covering the f-MWCNT's surface. –COOH functional groups on the f-MWCNT's surface may have reacted with the–OH groups on the Ti precursor through esterification to form O=C–O–Ti bonds. XPS spectra of a narrow scan of the O 1s region are shown in Figure 6B. The O 1s region can be deconvoluted into three different peaks. The peak at around 530.1 eV is attributed to the Ti–O–Ti bond of TiO_2, which means that the chemical state of the oxygen is the same as the chemical state of the main lattice oxygen in TiO_2. The other peaks were located at around 531.9 eV and were assigned to the binding energy of the C=O and hydroxyl group of C-OH at around 533 eV. Figure 6C shows two typical peaks located at binding energies of 459.2 eV and 464.8eV,

which were assigned to Ti 2p3/2 and Ti 2p1/2, being in agreement with the value of Ti^{4+} in the TiO_2 lattice [32]. It was observed that two peaks of Ti 2p were slightly shifted up compared with pure TiO_2.

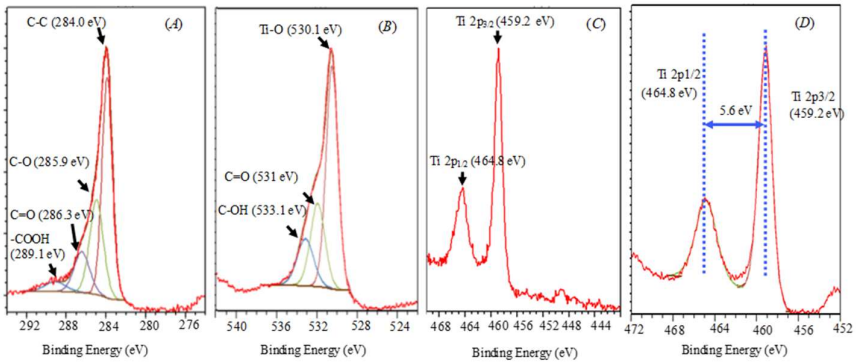

Figure 6 Deconvoluted XPS spectra of (A) C 1s, (B) O 1s, (C) Ti 2p, and (D). Deconvoluted XPS spectra of the Ti 2p region for sample D.

Theoretically, the TiO_2 bonding energies (Ti2p 3/2 and Ti2p 1/2) are centered at 458.4 and 464.2 eV with their difference being 5.8 eV [33]. The shifting indicates that the Ti atom present in TiO_2 coated f-MWCNT has a different chemical environment compared with Ti present in pure TiO_2. This is probably due to strong interaction between the TiO_2 and the f-MWCNT through Ti-O-C formation. A small positive displacement was observed, suggesting that the electronic interaction between the TiO_2 and the f-MWCNT substrate has a close interaction with the nanotubes and the TiO_2 [34]. Combining the XPS spectra and the fitting curves of C 1s and O1s indicated the presence of Ti-O-C bonds in the Ti-O area. The TiO_2 coating the f-MWCNT's surface indicates that there was good interaction between the TiO_2 and the f-MWCNT through Ti-O-C bonds, as found previously by Cong Ye, *et al.* [35]. In this case, interfacial charge transfers of TiO2/f-MWCNT nanocomposite are very likely to occur, wherein f-MWCNT inhibits the electron-hole recombination.

4 Conclusion

In this study, we successfully synthesized a hybrid nanocomposite of f-MWCNT-TiO_2 by microwave heating irradiation. The weight ratio of f-MWCNT-TTIP precursor is crucial in controlling the TiO_2 crystal size and phases. A high ratio of TTIP results in large-size and dense growth of TiO_2 particles on the f-MWCNT's surface. The results showed that anatase significantly influenced the

photocatalytic activity. The TiO_2-f-MWCNT nanocomposite had strong interaction through Ti-O-C bond formation.

Acknowledgments

This work was supported by Indonesian Institute of Sciences, National Priority Program Fiscal Year of 2021 and the Research Center for Physics-LIPI.

Reference

[1] Ibrahim, K.S., *Carbon Nanotubes-Properties and Applications: A Review*, Carbon Lett, **14**(3), pp. 131-144, 2013.

[2] Shimizu, A., Kato, H., Sato, T. & Kushida, M., *Preparation and Characterization of Oriented Poly (Vinyl Alcohol)/Carbon Nanotube Composite Nanofibers*, Jpn J Appl Phys, **56**, pp. 1-6, 2017.

[3] Yudianti, R., Onggo, H., Indriyati & Sudirman, *Role of Catalytic Synthesis On Growth and Distribution of Platinum Nanoparticle on Carbon Nanotube Surface*, Nanosci Nanotechno, **2**(6), pp. 171-177, 2012.

[4] Sudirman, Indriyati, Adi, W.A., Yudianti, R. & Budianto, E., *Structural Analysis of Platinum Nanoparticles on Carbon Nanotube Surface as Electrocatalyst System*, Int J Chem, **9**(2), pp. 60-66, 2017.

[5] Carp, O., Huisman, C.L. & Reller, A., *Photoinduced Reactivity of Titanium Dioxide*, Prog Solid State Chem, **32**(1-2), pp. 33-177, 2004.

[6] Anpo. M., *Utilization of TiO_2 Photocatalysts in Green Chemistry*, Pure Appl Chem, **72**(7), pp. 1265-1270, 2007.

[7] Tang, R., Jiang, Q. & Liu, Y., *Preparation and Study On Photocatalytic Activity of N-doped TiO_2 Decorated N-Doped Graphene*, Procedia Eng, **205**, pp. 573-580, 2017.

[8] Alosfur, F., Jumali, M.H.H., Radiman, S., Ridha, N.J., Yarmo, M.A. & Ali, A., *Visible Light-responsive TiO_2 coated MWCNTs as a Hybrid Nanocatalysts*, Int J Electrochem Sci, **8**, pp. 2977-2982, 2013.

[9] Divya, K.S., Athulya, K.M., Umadevi, T.U., Suprabha, T. & Suresh, M., *Improving the Photocatalytic Performance of TiO_2 via Hybridizing with Graphene*, J Semicond, **38**(6), 063002, 2017.

[10] Giovannetti, R., Rommozzi, E., Zannotti, M. & D'Amato, C.A., *Recent Advances in Graphene Based TiO_2 Nanocomposites ($Gtio_2ns$) for Photocatalytic Degradation of Synthetic Dyes*, Catalysts, **305**(7), pp. 2-34, 2017.

[11] Potirak, P., Pecharapa, W. & Techitdheera, W., *Microwave-assisted Synthesis of ZnO/MWCNT Hybrid Nanocomposites and Their Alcohol-Sensing Properties,* J Exp Nanosci, **9**(1), pp. 96-105, 2014.

[12] Chien-Te, H., Yu-Chia, C., Yu-Fu, C., Mohammad, M.H. & Po-Yen, C.B-S.J., *Microwave Synthesis of Titania-Coated Carbon Nanotube*

Composites For Electrochemical Capacitors, J Power Sourc, **269**, pp. 526-533, 2014.

[13] Bin, G.G., George, Z.C. & Puma, I.G., *Carbon Nanotubes/Titanium Dioxide (Cnts/Tio₂) Nanocomposites Prepared by Conventional and Novel Surfactant Wrapping Sol-Gel Methods Exhibiting Enhanced Photocatalytic Activity*, Appl Catal B Environ, **89**, pp. 503-209, 2009.

[14] Teck, C., *Progress in Polymer Science Nanofiber Technology: Current Status and Emerging Developments*, Prog Polym Sci, **70**, pp. 1-17, 2017.

[15] Ashkarran, A.A., Fakhari, M., Hamidinezhad, H., Haddadi, H. & Nourani, M.R., *TiO_2 Nanoparticles Immobilized on Carbon Nanotubes for Enhanced Visible-Light Photo-Induced Activity*, J Mater Res Technol, **4**(2), pp. 126-32, 2015.

[16] Nguyen, M.T., Nguyen, C.K., Vu, T.M.P., Van Duong, Q., Pham, T.L. & Nguyen, T.C., *A Study on Carbon Nanotube Titanium Dioxide Hybrids: Experiment and Calculation*, Adv Nat Sci Nanosci Nanotechnol, **5**(4), pp. 0-6, 2014.

[17] Hao, L., Miyazawa, K., Yoshida, H. & Lu, Y., *Visible-Light-Driven Oxygen Vacancies and Ti^{3+} Co-Doped TiO_2 Coatings Prepared by Mechanical Coating and Carbon Reduction*, Mater Res Bull, **97**, pp. 13-18, 2018.

[18] Guo, W., Liu, X., Huo, P., Gao, X., Wu, D., Lu, Z. & Yan, Y., *Hydrothermal Synthesis Spherical TiO_2 and Its Photo-Degradation Property on Salicylic Acid*, Appl Surf Sci, **258**(18), pp. 6891-6896, 2021.

[19] Archaapinun, K., Witit-anun, N. & Visuttipitukul, P., *Effect of Heat Treatment on Phase Transformation of TiO_2 and Its Reflectance Properties*, J Met Mater Miner, **23**(2), pp. 43-49, 2013.

[20] Yudianti, R., Onggo, H., Sudirman, Saito, Y., Iwata, T. & Azuma, J., *Analysis of Functional Group Sited on Multi-Wall Carbon Nanotube Surface*, Open Mater Sci J, **5**(1), pp. 242-247, 2011.

[21] Abdullahi, N., Saion, E., Shaari, A.H., Al-Hada, N.M. & Keiteb, A., *Optimisation of The Photonic Efficiency of TiO_2 Decorated on MWCNTs for Methylene Blue Photodegradation*, PLoS One, **10**(5), pp. 1-12, 2015.

[22] Kuvarega, A.T. & Mamba, B.B., *Double Walled Carbon Nanotube/Tio₂ Nanocomposites for Photocatalytic Dye Degradation*, Nanomater J, 2016.

[23] Bhattacharya, P., Sahoo, S. & Das, C.K., *Microwave Absorption Behaviour of MWCNT Based Nanocomposites in X-Band Region*, Express Polym Lett, **7**(3), pp. 212-213, 2012.

[24] Galizia, P. & Maizza, G., *Heating Rate Dependence of Anatase to Rutile Transformation,* Process Appl Ceram, **10**(4), pp. 235-241, 2016.

[25] Dai, S., Wu, Y., Sakai, T., Du, Z., Sakai, H. & Abe, M., *Preparation of Highly Crystalline TiO_2 Nanostructures by Acid-Assisted Hydrothermal Treatment of Hexagonal-Structured Nanocrystalline Titania/ Cetyltri-*

methyammonium Bromide Nanoskeleton, Nanoscale Res Lett, **5**, pp. 1829-1835, 2010.

[26] Byrne, C., Fagan, R., Hinder, S., McCormack, D.E. & Pillai, S., *New Approach of Modifying the Anatase to Rutile Transition Temperature in TiO2 Photocatalysts,* RSC Adv J, **6**, pp. 95232-95238, 2016.

[27] Spiridonova, J., Katerski, A., Danilson, M., Krichevskaya, M., Krunks, M. & Acik, I.O., *Effect of the Titanium Isopropoxide : Acetylacetone Molar Ratio on thephotocatalytic activity of TiO_2, Molecule,* **24**, pp. 1-14, 2019.

[28] Lourduraj, S. & Williams, R.V., *Effect of Molarity on Sol-Gel Routed Nano TiO_2 Thin Films*, J Adv Dielectr, **7**(6), pp. 1-7, 2017.

[29] Kamaluddin, M.R., Zamri, N.I.I., Kusrini, E., Prihandini, W.W., Mahadi, A.H. & Usman, A., *Photocatalytic Activity of Kaolin–Titania Composites to Degrade Methylene Blue Under UV Light Irradiation; Kinetics, Mechanism and Thermodynamics*, React Kinet Mech Catal, **133**, pp. 517-529, 2021.

[30] Zulmajdi, S.L.N., Zamri, N.I.I., Yasin, H.M., Kusrini, E., Hobley, J. & Usman, A., *Comparative Study on the Adsorption, Kinetics, And Thermodynamics of the Photocatalytic Degradation of Six Different Synthetic Dyes on TiO2 Nanoparticles*, React Kinet Mech Catal, **129**, pp. 519-534, 2020.

[31] Carrera, R., Castillo, N., Arce, E., Vazquez, A.L., Moran-Pineda, M., Montoya, J.A., Del Angle, P. & Castillo, S., *Analysis of Polymorphic Nanocrystals of TiO_2 By X-Ray Rietveld Refinement and High-Resolution Transmission Electron Microscopy: Acetaldehyde Decomposition*, Res Lett Nanotechnol, pp. 1-5, 2008.

[32] Liu, C., Zhang, L., Liu, R., Gao, Z., Yang, X. & Tu, Z., *Hydrothermal Synthesis of N-doped TiO_2 Nanowires and N-doped Graphene Heterostructures with Enhanced Photocatalytic Properties*, J Alloys Compd, **656**, pp. 24-32, 2016.

[33] Vargas, H.J., *Structural and Morphological Modification of TiO_2 Doped Metal Ions and Investigation of Photo-Induced Charge Transfer Processes*, Ph.D. Thesis, Institut des Molécules et Matériaux du Mans, France, 2017.

[34] Li, J., Tang, S., Lu, L. & Zeng, H.C., *Preparation of Nanocomposites of Metals, Metal Oxides, and Carbon Nanotubes via Self-Assembly*, J Am Chem Soc, **129**(30), pp. 9401-9409, 2007.

[35] Cong, Y., Li, X. & Qin, Y.D.Z., *Carbon-doped TiO_2 Coating on Multiwalled Carbon Nanotubes with Higher Visible Light Photocatalytic Activity*, Appl Catal B Environ, **107**(1-2), pp. 128-134, 2011.